Geophysical Research Letters

RESEARCH LETTER
10.1029/2021GL096691

Key Points:

- Ionospheric conditions before substorm onset are different for substorms with an early local time onset versus late local time onset
- Substorm onsets tend to move to earlier local times with increasing geomagnetic activity
- We suggest that higher ionospheric conductance leads to a duskward shift in magnetospheric substorm activity

Correspondence to:

R. Elhawary,
reham.elhawary@uib.no

Citation:

Elhawary, R., Laundal, K. M., Reistad, J. P., & Hatch, S. M. (2022). Possible ionospheric influence on substorm onset location. *Geophysical Research Letters*, *49*, e2021GL096691. https://doi.org/10.1029/2021GL096691

Received 22 OCT 2021
Accepted 9 FEB 2022

Author Contributions:

Supervision: K. M. Laundal, J. P. Reistad
Writing – review & editing: K. M. Laundal, J. P. Reistad, S. M. Hatch

Possible Ionospheric Influence on Substorm Onset Location

R. Elhawary[1], K. M. Laundal[1], J. P. Reistad[1], and S. M. Hatch[1]

[1]Birkeland Centre for Space Science, University of Bergen, Bergen, Norway

Abstract Auroral substorm onset locations are highly unpredictable. Previous studies have shown that the B_y component of the interplanetary magnetic field (IMF) explains ∼5% of the variation in onset magnetic local time (MLT), while solar wind conditions and the other IMF components have even less explanatory power. In this study, we show that the level of geomagnetic activity before substorm onset, as indicated by the AL index, explains an additional ∼5% of the variation in onset MLT. We discuss our results with regard to recent modeling studies, which show that gradients in the ionospheric Hall conductance can lead to a duskward shift of the magnetotail dynamics. Our findings suggest that this magnetosphere-ionosphere coupling effect may also influence the location of substorm onsets.

Plain Language Summary Substorms are explosive disturbances in our magnetotail that impact the earth's ionosphere. They happen on average several times per day and as a result of this phenomenon, we can see the marvelous aurora. Substorms happen on the nightside of the earth and can take place over a wide range of latitudes and longitudes. In this study, we show that substorms tend to begin at earlier local times during geomagnetically active times than during quiet times. We interpret this tendency as a sign that ionospheric conditions may play a role in determining where substorms occur.

1. Introduction

Substorms are abrupt global-scale changes in the magnetotail that release the energy stored in the nightside magnetosphere into the two nightside polar ionospheres via field-aligned currents and particle precipitation. Akasofu (1964) defined the substorm in terms of two phases, the expansion phase, and the recovery phase. Later McPherron (1970) defined a third phase of the substorm, the growth phase. The growth phase of the substorm is the period before the onset of the expansion phase, typically lasting for 30–60 min (Lui, 1991), when kinetic energy in the solar wind is transferred to magnetic energy in the magnetotail and then thermal energy in the plasma sheet. During the expansion phase, the aurora suddenly becomes bright and evolves into a global distribution in typically 10–30 min. Finally, a recovery phase can last for more than 2 hr. See, for example, McPherron and Chu (2016) for a detailed review about the development of the definition of substorms.

The substorm cycle is an integral component of solar wind-magnetosphere-ionosphere coupling: Substorms are the central process by which the magnetosphere releases magnetic flux opened on the dayside back into the solar wind through reconnection in the neutral sheet of the magnetotail (Milan et al., 2010). Substorms also release energy in the magnetotail that reorganizes ionospheric flows (Grocott et al., 2017).

Global UV images of the aurora have shown that 80% of substorm onsets (i.e., between the 10th and 90th percentile) happen in a ∼3.2 hr wide range of magnetic local time (MLT), centered pre-midnight (Frey et al., 2004; Liou, 2010). It may not be surprising that substorm auroras take place at pre-midnight, given that the upward current at the duskward edge of the substorm current wedge (SCW) should be associated with downward electrons. However, we believe that the onsets listed by Frey et al. (2004); Liou (2010) occur before the SCW is developed (Kepko et al., 2015) and the structure of the SCW probably does not explain the duskward shift. Furthermore, the onset aurora may not be closely associated with FACs at all (Mende et al., 2003), but instead, map to the transition between the dipolar and the stretched field lines. Beyond this statistical distribution, the location of substorm onsets remains largely unpredictable. Previous studies have attempted to predict the location of the substorm onset by correlating the MLT and magnetic latitude (MLat) of the substorm onset with different parameters. For instance, Liou et al. (2001) found that substorms occur at lower latitudes when the interplanetary magnetic field (IMF) B_z component is negative, compared to positive. Gérard et al. (2004) also found a correlation between MLat of the substorm onset and solar wind dynamic pressure. Both effects may be the result of relatively more open flux in the magnetosphere, which moves the auroral oval equatorward (Milan et al., 2009).

Many other studies have shown that the substorm onset MLT depends on the polarity of IMF B_y rather than IMF B_z (Liou & Newell, 2010; Østgaard et al., 2004, 2005, 2011; Wang et al., 2007). Using the lists of substorm onsets based on global UV imaging by Frey et al. (2004) and Liou (2010), Østgaard et al. (2011) showed that the substorm onset MLT and IMF B_y are correlated. Though the relationship between IMF B_y and substorm onset MLT is statistically significant, IMF B_y only explains 5% of the variation of the substorm onset MLT. Tenfjord et al. (2015) argued that the asymmetric addition of open flux during IMF B_y periods leads to an induced B_y in the magnetosphere, which in turn can lead to changes in the observed projection of the substorm onset on the ionosphere. This projection effect may explain the observed variation of onset location versus IMF B_y. Furthermore, simultaneous observations of substorm onsets in the two hemispheres show that the correlation of the relative shift in MLT with IMF B_y is much higher (Østgaard et al., 2005), consistent with our interpretation that the IMF B_y effect is due to a relative shift of the onset MLT in each hemisphere (i.e., an effect of field line mapping), and not a real shift of the onset location in the magnetosphere. In addition to IMF B_y, the dipole tilt angle may also have a similar effect on the observed onset location in the ionosphere: Due to tail warping associated with nonzero dipole tilt (e.g., Tsyganenko, 1998), a positive dipole tilt angle will lead to an added positive B_y component on closed field-lines in the magnetotail at dusk, and an added negative B_y component at dawn (e.g., Liou & Newell, 2010; Figure 3). This perturbation field would project phenomena in the dusk magnetotail to earlier (later) local times in the northern (southern) ionosphere. Substorm onset statistics presented by Liou and Newell (2010) and Østgaard et al. (2011) are consistent with this idea, assuming that most onsets happen at dusk in the magnetotail.

The results presented in these previous studies may be completely explained by mapping effects, while the location of the onset in the magnetotail remains unpredictable. The observed shift toward dusk of the typical onset location is similar to the observed distribution of tail reconnection (e.g., Angelopoulos et al., 1994; Kiehas et al., 2018). One potential explanation of this shift is related to the Hall effect in a thin current sheet. This was investigated by Lu et al. (2016) and Lu et al. (2018), who conducted a hybrid 3D global simulation and a particle in a cell simulation, respectively, with uniform ionospheric conductances to exclude the ionospheric effects. They found that the Hall effect is stronger on the dusk side due to higher ion perpendicular temperature, and a smaller B_z. Another potential explanation that includes the ionospheric contribution to the observed shift was presented in Lotko et al. (2014). They performed three MHD simulations: In the first simulation, they introduced uniform ionospheric conductance and observed symmetric magnetotail activity. In the second simulation, they introduced high Hall conductance in the auroral oval and monitored the magnetotail activity which shifted toward dusk. In the third simulation, they introduced an unrealistic depression in Hall conductance in the auroral oval and monitored the magnetotail activity which shifted toward dawn. The results of Lotko et al. (2014) suggest that ionospheric feedback influences the duskward shift of tail reconnection and, possibly, substorm onsets. In the current paper, we test this idea using observations of substorm onsets, ground magnetic field perturbations, and solar wind conditions.

2. Observations

We use the Frey et al. (2004) and Liou (2010) lists to investigate substorm onsets in this study. The two lists combined have 6,192 substorms in the period 1996–2005, with 4,762 substorms observed in the Northern hemisphere and 1,430 substorms observed in the Southern hemisphere. The substorm onsets identified in Frey et al. (2004) as "a clear local brightening of the aurora." Two additional criteria have been applied to identify the substorm onset in this list: After observing the clear local brightening, they require (a) that the expansion of the aurora lasts for at least 20 min, (b) that the poleward expansion goes over the poleward boundary of the oval, and (c) that the onset occurs at least 30 min after a previously identified onset. In the list provided by Liou (2010), the substorm onset is identified as "a sudden brightening of the aurora." The author then uses the same criteria as Frey et al. (2004) except that in the second step, he does not require the poleward expansion to go beyond the poleward boundary of the oval. Afterward, the identified images related to substorm events are transformed to geomagnetic coordinate system to provide the onset MLT and MLat.

To investigate whether the ionospheric state may possibly influence substorm onset location, we used the magnitude of the horizontal geomagnetic data from the northern hemisphere (ground B) $= \sqrt{< E_{qd}^2 + N_{qd}^2 >}$ where E_{qd} and N_{qd} are the eastward and northward component of the magnetic field in quasi-dipole coordinates. The ground magnetic field perturbations were obtained from the SuperMAG database in geographic

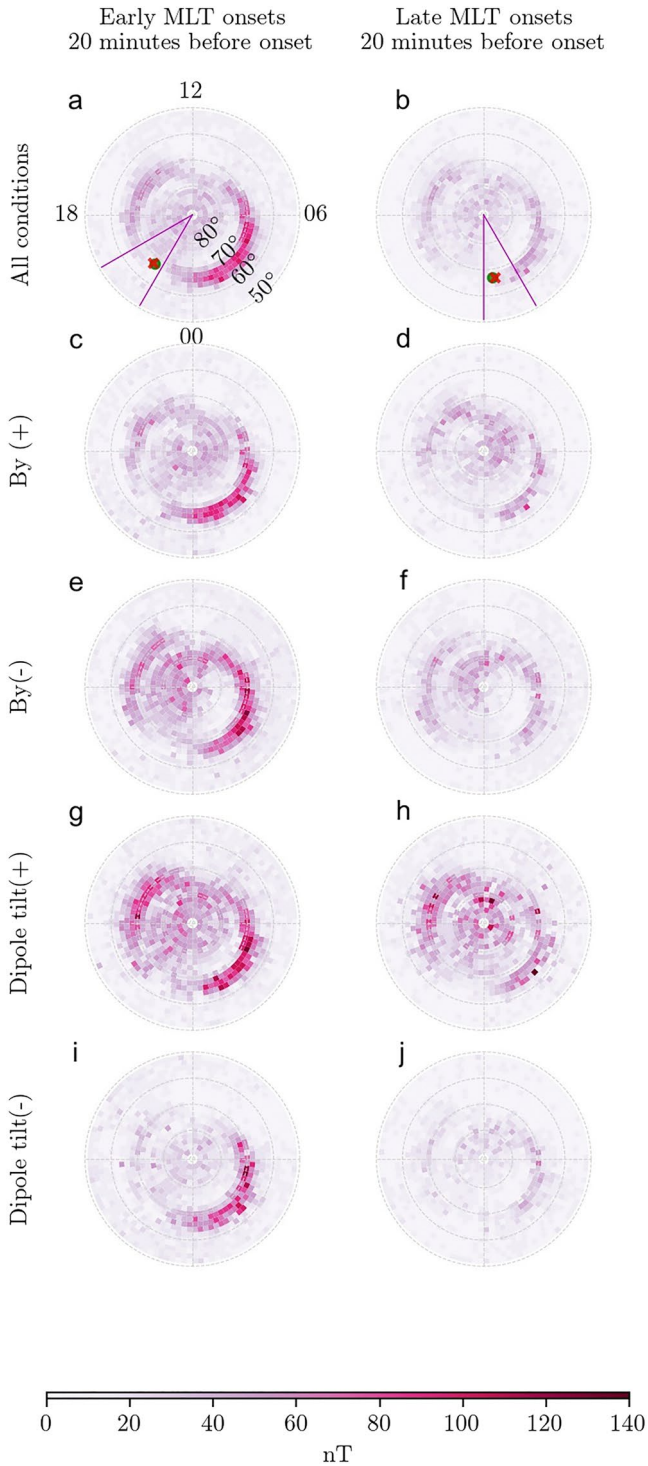

Figure 1. Maps of the magnitude of the average horizontal magnetic field perturbations (ground B) 20 min before the substorm onset. The left column shows onsets observed between 20 and 22 MLT (early) and the right column shows onsets observed between 24 and 02 MLT (late). Panels a and b show maps of early and late onsets based on all the available data. Panels c and d (e and f) show early and late onsets that occurred when IMF B_y was positive (negative). Panels g and h (i and j) show maps for positive (negative) dipole tilt angle. Each panel uses an equal-area grid with 2° MLat resolution.

coordinates with the baseline subtracted as described in Gjerloev (2012). The data is then converted to quasi-dipole coordinates following Laundal et al. (2016). Figure 1 shows maps of the magnitude of (ground B). The colors represent the median ground B perturbations magnitude 20 min before substorm onsets for different conditions of IMF B_y and dipole tilt angle.

The left column shows onsets observed between 20 and 22 MLT (hereafter "early onsets") and the right column shows onsets observed between 24 and 02 MLT (late onsets), as the distribution of the substorm onsets is centered around 23 MLT (Gérard et al., 2004; Liou & Newell, 2010). Figures 1a and 1b show the median magnetic field perturbations 20 min before early and late substorm onsets, respectively. The magenta lines are the boundaries of the onset locations. The red cross × is the location of the mean onset location while the green circle • is the median. The median MLT of the early (late) subset is 21.47 (0.54). We find that the magnitude of ground B is generally higher during the 20 min preceding early substorm onsets than during the 20 min preceding late substorm onsets.

The separation into early and late onsets biases the distributions of IMF B_y and dipole tilt angle since we know that these parameters influence the onset location. To ensure that this bias is not the reason for the different ground B magnitudes, we further separate the onsets by the sign of IMF B_y and dipole tilt angle. Panels (c–f) of Figure 1 show maps of ground B for early and late onsets with the different polarity of IMF B_y, and $|B_y| > 1$ nT. We used measurements of IMF B_y with a 1-min resolution provided from the OMNI data set, time shifted to the bow shock. We use the median during the 20 min before the substorm onset. For both polarities of IMF B_y, the magnitude of ground B for early onset substorms is higher than the magnitude for late-onset substorms. Panels (g–j) of Figure 1 show maps of ground B for substorms that occurred at times with different dipole tilt angle Ψ (Laundal & Richmond, 2017). For both signs of the dipole tilt angle, the magnitude of ground B is higher for early substorms than late substorms. These panels show that the bias in B_y and Ψ is not the reason for the different B magnitudes in the two columns.

Motivated by our results showing profound differences in the ionospheric state before early and late substorm onsets, we have examined the relationship between substorm onset MLT and four different parameters: The auroral lower (AL) index, the solar wind aberration angle, the dipole tilt angle, and IMF B_y. For all variables except for dipole tilt angle, we use the mean value during the 60 min before onset. Figures 2a–2d show the results of a regression analysis of MLT and each of these variables separately. In each panel, the regressor is divided into 10 bins with an equal number of observations, and the median onset MLT is shown in blue (red) for substorms observed in the northern (southern) hemisphere. The vertical bars represent the standard error of the median (see, e.g., Greene, 2003, page 878; not the standard deviation). The dashed lines represent regression models to be discussed in more detail below. Figure 2e shows the result of a multivariable regression analysis where all four parameters are combined and will be explained below. We have also examined the relationship between the substorm onset MLT and IMF B_z. The median IMF B_z for early and late MLT onsets is −1.8 and −1.5 nT, respectively. This result is consistent with Liou et al. (2001), who found that there is no clear relationship between IMF B_z and variations of the MLT of the substorm onsets. That IMF B_z is not strongly related to the onset MLT, while the AL index is, is counter-intuitive because the IMF B_z and AL are

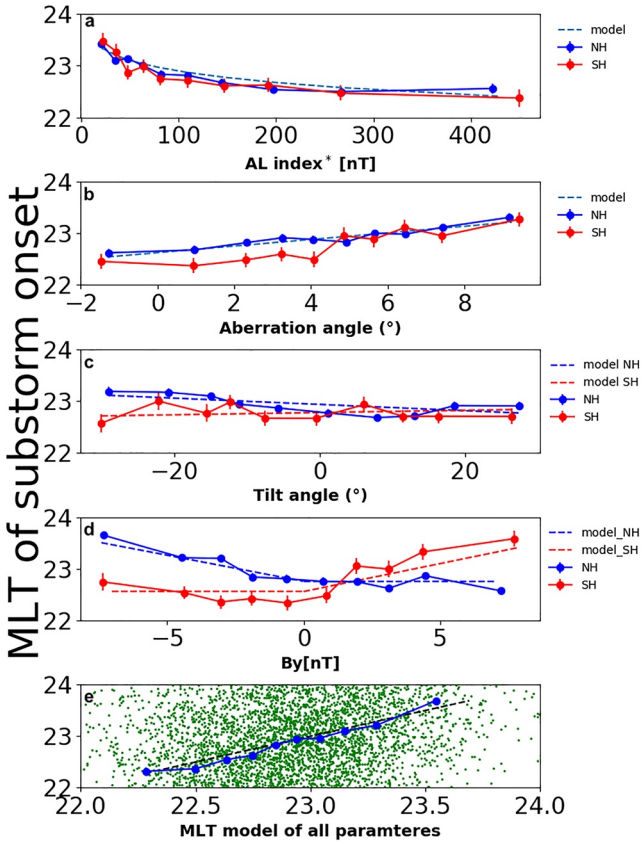

Figure 2. Panels (a–d) shows the relationship between the substorm onset MLT and the AL index, the aberration angle, the dipole tilt angle, and IMF B_y respectively, panel (e) shows the multivariable regression analysis with the four parameters. Each substorm onset from the combined lists is plotted against the model prediction as green dots. The black dashed line represents where the data would be in the ideal case that the model makes perfect predictions. Our model follows the dashed line closely.

correlated. However, the AL index is not a simple function of the simultaneous B_z, but also depends on the delayed response of the magnetotail to energy transfer from the solar wind to the magnetosphere (Laundal et al., 2020). Our results therefore indicate that the possible ionospheric influence on substorm onset location depends more on the time-delayed magnetotail component.

Figure 2a shows the relationship between the onset MLT and the AL index. The purpose of analyzing the variation between onset MLT and the AL index is to quantify the effect that is observed in Figure 1, that stronger magnetic field perturbations before a substorm are associated with earlier onset MLTs. The AL index measures the maximum strength of the westward electrojet from 12 magnetometers longitudinally distributed along the auroral oval, and is here taken as a proxy of geomagnetic activity. The x-axis of Figure 2a represents a modified AL, AL*, defined as max(AL) - AL, where max(AL) is the maximum value of AL = 7.85 nT. This ensures that AL* is always positive. We see from Figure 2a that the variation of substorm onset MLT as a function of AL is nonlinear. We therefore seek a regression model on the form $y = a - b\mathrm{AL}^{*\gamma}$, where y is the onset MLT and a, b, and γ are model parameters to be fitted. Since AL* is positive, y will be real for all γ. The model parameters are estimated using non-linear least squares, with all data points individually (not the median values). The resulting model parameters are a = 25.7 hr, b = 1.69 hr/nT, and γ = 0.1. The coefficient of determination (the square of the correlation coefficient) r^2 is 0.049, which means that the model explains about 4.9% of the variation of the substorm onset MLT, roughly the same as IMF B_y-based statistical models (see Østgaard et al., 2011, and below). In contrast to variation with IMF B_y, the variation with AL is in the same direction in both hemispheres.

Figure 2b shows the relationship between the aberration angle and the MLT of the substorm onset. The aberration angle α is the angle between the Sun-Earth line and the solar wind velocity as defined by (Hones et al., 1986). We calculate the aberration angle as $\alpha = \tan^{-1}(-V_y/V_x)$, where V_y is the solar wind velocity in the GSM y-direction. The V_y provided by OMNI is given in an inertial frame, but we have converted to an Earth fixed frame by adding Earth's orbital speed, 29.8 km/s. We expect that the onset MLT varies linearly with aberration angle, since the magnetosphere aligns with the solar wind velocity (a "windsock effect"). This is also supported by the medians in Figure 2b. We therefore seek a model on the form $y = a + b\alpha$. We estimated model parameters are a = 22.6 hr and b = 0.96, when the angle α is given in hours. The fact that b is so close to 1 is in agreement with the expected windsock effect. The coefficient of determination is 2.5%.

Figure 2c shows the relationship between the dipole tilt angle Ψ and the MLT of the substorm onset. We see that the onset MLT decreases (increases) with dipole tilt angle in the Northern (Southern) hemisphere. The figure indicates that the relationships are linear, so we seek models on the form $y_{n,s} = a_{n,s} + b_{n,s}\Psi$, where the subscripts refer to the Northern and Southern hemispheres. We find that $a_n(a_s)$ = 22.9(22.7) and $b_n(b_s)$ = − 0.006(0.002) hr/degree. In both cases, the models explain less than 1% of the substorm onset MLT variation. However, since the number of samples is so large, the probability that this would occur by chance is less than 10^{-8}. In the other regression models, the correlation is higher, and the p value is smaller.

Figure 2d shows the relationship between the IMF B_y component of the solar wind and the MLT of the substorm onset. Milan et al. (2010) suggested that for IMF B_y to impact the onset MLT, the polarity must be the same for a long time prior to the substorm onset. In our analysis, we used the mean of IMF B_y 1 hr before the substorm onset. We see that if IMF B_y is negative (positive), the substorm onsets tend to be observed at later (earlier) local times in the northern (southern) hemisphere. For the opposite sign, the variation is minimal. This is in agreement with the results by Østgaard et al. (2011). Because of this, we seek regression models of the form

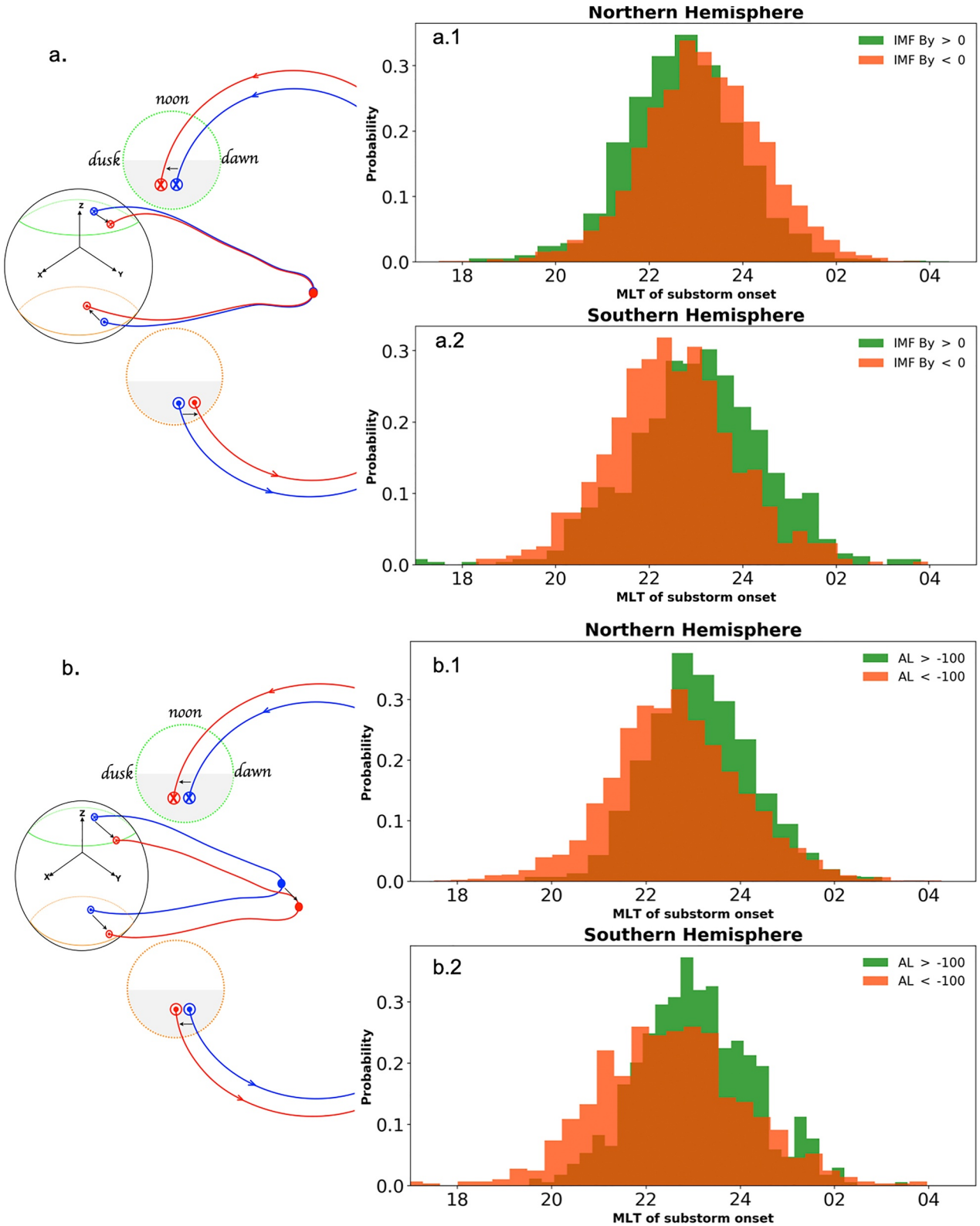

Figure 3.

$$y_n = \begin{cases} a_n + b_n B_y & \text{if } B_y < 0 \\ a_n & \text{if } B_y \geq 0, \end{cases}, \quad (1)$$

and for the southern hemisphere,

$$y_s = \begin{cases} a_s & \text{if } B_y < 0 \\ a_s + b_s B_y & \text{if } B_y \geq 0, \end{cases}. \quad (2)$$

We find that $a_n(a_s) = 22.75(22.55)$ h, and $b_n(b_s) = 0.11(-0.10)$ hr/nT. Both models explain about 4.5% of the variation in onset MLT.

Figure 2e shows the result of a multivariable regression analysis which includes all the above parameters. The multivariable model combines all the above model representations, and the model parameters are coestimated. In this model, we reverse the signs of B_y and dipole tilt angle Ψ for substorms observed in the Southern hemisphere. The resulting model is $y = 24.63–0.10B_y - 1.14AL^{*0.13} - 0.0035\Psi + 0.66\alpha$, where B_y and AL are given in nT, Ψ in degrees, and α in hours. Figure 2e shows each onset plotted against the model prediction as green dots. The dashed line represents where the data would be in the ideal case that the model makes perfect predictions. However, the model only captures 11.3% of the total variance of the MLT of the substorm onsets. The individual data points (green dots) are included in this panel to highlight the large degree of scatter. The standard deviation of the full onset MLT distribution is 1.3 hr, and several substorms also occur outside the bounds of this plot. In the panels above, only binned medians are shown, although the individual data points were used in the regression analyses. The blue dots in Figure 2e also represent binned medians, in 10 bins based on model prediction quantiles, and we see that they follow the dashed line closely. The standard error of the median is too small to be noticed.

3. Discussion and Summary

We have shown that substorm onsets tend to occur at earlier local times during geomagnetically active periods relative to substorm onsets during quiet periods. The regression analyses presented in Figures 2a and 2d show that the AL index before substorm onset is as strongly correlated with onset MLT as the IMF B_y, which has been reported in several earlier studies (Liou & Newell, 2010; Østgaard et al., 2011; Wang et al., 2007).

A key difference from the effect of IMF B_y is that the onset MLT dependence is the same in the two hemispheres with respect to AL. Since the effect of IMF B_y is opposite in the two hemispheres, and since it only explains about 5% of the observed variation in onset MLT, we interpret it as an effect of magnetic mapping. That is, IMF B_y does not influence the location of the substorm onset in the magnetotail, only how it maps to the ionosphere, where we see the auroral emissions. The IMF B_y induces a B_y component in the magnetosphere with the same sign (Tenfjord et al., 2015), which causes the observed substorm onsets to shift in opposite directions in the two hemispheres. This mapping effect is illustrated in Figure 3a. The blue magnetic field line is symmetric between the two hemispheres, and the red magnetic field line illustrates what happens when we introduce a positive B_y in the magnetotail: The footpoint shifts toward dusk in the northern hemisphere and toward dawn in the southern hemisphere. Figure 3a1 (a.2) shows the distribution of substorm onset locations observed in the northern (southern) hemisphere under B_y positive (green) and negative (orange) conditions. We calculated IMF B_y as the

Figure 3. Conceptual figure illustrating (a) the mapping effect and (b) the real shift in the magnetotail. In panels (a) and (b), the green (orange) circle represents the northern (southern) hemisphere's high latitude ionosphere, the blue line is a magnetic field line to be shifted toward either dawn or dusk, appearing as the red line after the shift. The shift is in opposite direction between the northern and southern hemispheres in (a) and in the same direction in (b) Panels (a1) and (a2) represent the distributions of the MLT of substorm onsets in Northern and Southern hemisphere, respectively, the panels show that the substorm onset MLT distribution observed in the northern (southern) hemisphere with positive IMF B_y shifts toward earlier (later) MLT. Panels (b1) and (b2) represent the distributions of the MLT of substorm onsets in Northern and Southern hemisphere, respectively. The panels show that the substorm onset MLT observed in both northern and southern hemispheres shift toward earlier local time in both hemispheres for increased AL.

mean during 1 hr before the substorm onset as used in the linear regression analysis above. We see that the effect is in the opposite direction in the two hemispheres.

Figure 3b illustrates our interpretation of the onset MLT dependence on the AL index: Since the shift is in the same direction in both hemispheres, it is presumably not an effect of mapping, as with IMF B_y. Instead of a mapping effect, there is a real shift of substorm onset location in the magnetotail toward dusk when geomagnetic activity increases. The blue magnetic field line in Figure 3b represents a quiet time situation, and the red magnetic field line represents active times. Figures 3b1 and 3b2 show the distribution of substorm onset locations observed in the northern hemisphere and the southern hemisphere respectively for high (green) and low (orange) activity, quantified in terms of the AL index before the substorm onset. We see that the effect is in the same direction in the two hemispheres.

Two different mechanisms have been proposed to explain dawn-dusk asymmetries in nightside activity: (a) A duskward shift of the plasma convection in the ionosphere due to conductance gradients and associated influence on the magnetotail (Lotko et al., 2014), and (b) a duskward displacement of the tail reconnection region due to Hall effects (Lu et al., 2016, 2018). The two mechanisms are not mutually exclusive, and both may be relevant to understand our observations of an AL control on onset MLT. However, the ionospheric conductance effect is presumably more directly related to the AL index than the magnetotail Hall effect. Considering the ionospheric Ohm's law, the AL index and conductance are proportional; but the conductance can be high even if the magnetotail current sheet is not thin, and vice versa. The ionospheric conductance effect on global magnetospheric dynamics was investigated in detail by Lotko et al. (2014). They used a magnetohydrodynamic simulation of the magnetosphere, with an electrostatic coupling to the ionosphere. They performed three simulation runs using the same solar wind conditions, but three different high-latitude distributions of ionospheric conductance: First, a uniform ionospheric conductance produced symmetric magnetotail activity with respect to the Sun-Earth line. Second, a realistic, empirical distribution with enhanced Hall conductance in the auroral oval produced magnetotail activity shifted toward dusk. Third, an unrealistic distribution of artificially depressed Hall conductance in the auroral oval produced magnetotail activity shifted toward dawn. These simulations clearly illustrate that ionospheric feedback can impact magnetospheric dynamics, and in particular magnetotail reconnection. If, as suggested by Angelopoulos et al. (2008), substorms are triggered by tail reconnection, it is likely that the effect studied by Lotko et al. (2014) and Zhang et al. (2012) may influence the location of the substorm onset and the subsequent expansion.

Wolf (1970) and Atkinson and Hutchison (1978) showed that the conductance gradient associated with the sunlight terminator can imply a clockwise rotation of the ionospheric convection pattern. This rotation could be an additional contributing factor in the duskward shift of magnetospheric activity. However, unlike the auroral gradient effect studied by Lotko et al. (2014), the terminator gradient effect is not expected to change with increasing geomagnetic activity.

Earlier studies, for example, Rostoker (1991) have reported that consecutive auroral brightenings tend to appear at progressively earlier local times. This could be a manifestation of the same mechanism(s) responsible for the observed relationship between the substorm onset MLT and the AL index discussed in this study. Kiehas et al. (2018) related observed duskward shift in magnetotail plasma flow to the high geomagnetic activity of high AL index. They suggested that the near-Earth reconnection is favorably located at the dusk sector as suggested by Lotko et al. (2014), Lu et al. (2016, 2018), and Zhang et al. (2012).

The ionospheric effect observed in the simulations reported by Lotko et al. (2014) relies on electrostatic models to represent the magnetosphere-ionosphere coupling. In reality, this coupling is not electrostatic, and an electrostatic model cannot explain *how* ionospheric feedback causes the magnetospheric activity to shift toward dusk. Determining the process by which ionospheric feedback regulates magnetospheric activity requires solving the equations that describe conservation of mass and momentum for ions and electrons moving through the neutral fluid, as they respond to electromagnetic fields that obey Maxwell's equations (e.g., Dreher, 1997).

Even though we have shown that the AL index is as useful in predictions of substorm onset MLT as IMF B_y, the explanatory power of our regression models (Figure 2) are all very low. A model that combines IMF B_y, the AL index, the aberration angle, and the dipole tilt angle explains about 11% of the observed variation in substorm onset MLT. The timing and location of substorm onsets therefore remain highly unpredictable.

Data Availability Statement

Magnetometer data can be downloaded directly from https://supermag.jhuapl.edu/mag where you need to specify the year to download. In our case, we used the years between 1996 and 2005. Solar wind data can be downloaded from https://cdaweb.gsfc.nasa.gov/sp_phys/data/omni/hro_1min/.

Acknowledgments
This study was supported by the Research Council of Norway/CoE under contracts 223252/F50 and 300844/F50, and by the Trond Mohn Foundation. For the ground magnetometer data the authors gratefully acknowledge: INTERMAGNET, Alan Thomson; CARISMA, PI Ian Mann; CANMOS, Geomagnetism Unit of the Geological Survey of Canada; The S-RAMP Database, PI K. Yumoto and Dr. K. Shiokawa; The SPIDR database; AARI, PI Oleg Troshichev; The MACCS program, PI M. Engebretson; GIMA; MEASURE, UCLA IGPP and Florida Institute of Technology; SAMBA, PI Eftyhia Zesta; 210 Chain, PI K. Yumoto; SAMNET, PI Farideh Honary; IMAGE, PI Liisa Juusola; Finnish Meteorological Institute, PI Liisa Juusola; Sodankylä Geophysical Observatory, PI Tero Raita; UiT the Arctic University of Norway, Tromsø Geophysical Observatory, PI Magnar G. Johnsen; GFZ German Research Centre For Geosciences, PI Jürgen Matzka; Institute of Geophysics, Polish Academy of Sciences, PI Anne Neska and Jan Reda; Polar Geophysical Institute, PI Alexander Yahnin and Yarolav Sakharov; Geological Survey of Sweden, PI Gerhard Schwarz; Swedish Institute of Space Physics, PI Masatoshi Yamauchi; AUTUMN, PI Martin Connors; DTU Space, Thom Edwards and PI Anna Willer; South Pole and McMurdo Magnetometer, PI's Louis J. Lanzarotti and Alan T. Weatherwax; ICESTAR; RAPIDMAG; British Artarctic Survey; McMac, PI Dr. Peter Chi; BGS, PI Dr. Susan Macmillan; Pushkov Institute of Terrestrial Magnetism, Ionosphere and Radio Wave Propagation (IZMIRAN); MFGI, PI B. Heilig; Institute of Geophysics, Polish Academy of Sciences, PI Anne Neska and Jan Reda; University of L'Aquila, PI M. Vellante; BCMT, V. Lesur and A. Chambodut; Data obtained in cooperation with Geoscience Australia, PI Andrew Lewis; AALPIP, co-PIs Bob Clauer and Michael Hartinger; MagStar, PI Jennifer Gannon; SuperMAG, PI Jesper W. Gjerloev; Data obtained in cooperation with the Australian Bureau of Meteorology, PI Richard Marshall. The authors acknowledge as well the use of NASA/GSFC's Space Physics Data Facility's OMNIWeb service, and OMNI data.

References

Akasofu, S. I. (1964). The development of the auroral substorm. *Planetary and Space Science*, *12*(4), 273–282. https://doi.org/10.1016/0032-0633(64)90151-5

Angelopoulos, V., Kennel, C. F., Coroniti, F. V., Pellat, R., Kivelson, M. G., Walker, R. J., et al. (1994). Statistical characteristics of bursty bulk flow events. *Journal of Geophysical Research: Space Physics*, *99*(A11), 21257–21280. https://doi.org/10.1029/94JA01263

Angelopoulos, V., McFadden, J. P., Larson, D., Carlson, C. W., Mende, S. B., Frey, H., et al. (2008). Tail reconnection triggering substorm onset. *Science*, *321*(5891), 931–935. https://doi.org/10.1126/science.1160495

Atkinson, G., & Hutchison, D. (1978). Effect of the day night ionospheric conductivity gradient on polar cap convective flow. *Journal of Geophysical Research*, *83*, 725–729. https://doi.org/10.1029/ja083ia02p00725

Dreher, J. (1997). On the self-consistent description of dynamic magnetosphere-ionosphere coupling phenomena with resolved ionosphere. *Journal of Geophysical Research*, *102*, 85–94. https://doi.org/10.1029/96JA02800

Frey, H. U., Mende, S. B., Angelopoulos, V., & Donovan, E. F. (2004). Substorm onset observations by IMAGE-FUV. *Journal of Geophysical Research: Space Physics*, *109*(A10), 2. https://doi.org/10.1029/2004JA010607

Gérard, J. C., Hubert, B., Grard, A., Meurant, M., & Mende, S. B. (2004). Solar wind control of auroral substorm onset locations observed with the IMAGE-FUV imagers. *Journal of Geophysical Research: Space Physics*, *109*(A3), 1–13. https://doi.org/10.1029/2003JA010129

Gjerloev, J. W. (2012). The SuperMAG data processing technique. *Journal of Geophysical Research: Space Physics*, *117*(9), 1–19. https://doi.org/10.1029/2012JA017683

Greene, W. H. (2003). *Economic Analysis* (5th ed., pp. 1–1054). Pearson Education, Inc.

Grocott, A., Laurens, H. J., & Wild, J. A. (2017). Nightside ionospheric convection asymmetries during the early substorm expansion phase: Relationship to onset local time. *Geophysical Research Letters*, *44*(23), 11696–11705. https://doi.org/10.1002/2017GL075763

Hones, E. W., Zwickl, R. D., Fritz, T. A., & Bame, S. J. (1986). Structural and dynamical aspects of the distant magnetotail determined from ISEE-3 plasma measurements. *Planetary and Space Science*, *34*(10), 889–901. https://doi.org/10.1016/0032-0633(86)90001-2

Kepko, L., McPherron, R. L., Amm, O., Apatenkov, S., Baumjohann, W., Birn, J., et al. (2015). Substorm current wedge revisited. *Space Science Reviews*, *190*, 1–46. https://doi.org/10.1007/s11214-014-0124-9

Kiehas, S. A., Runov, A., Angelopolos, V., Hietala, H., & Korovinksiy, D. (2018). Magnetotail fast flow occurrence rate and dawn-dusk asymmetry at X_{GSM} -60 R_E. *Journal of Geophysical Research: Space Physics*, *123*(3), 1767–1778. https://doi.org/10.1002/2017JA024776

Laundal, K. M., Gjerloev, J. W., Østgaard, N., Reistad, J. P., Haaland, S., Snekvik, K., et al. (2016). The impact of sunlight on high-latitude equivalent currents. *Journal of Geophysical Research: Space Physics*, *121*(3), 2715–2726. https://doi.org/10.1002/2015JA022236

Laundal, K.-M., Reistad, J.-P., Hatch, S.-M., Moretto, T., Ohma, A., Østgaard, N., et al. (2020). Time-scale dependence of solar wind-based regression models of ionospheric electrodynamics. *Scientific reports*, *10*. https://doi.org/10.1038/s41598-020-73532-z

Laundal, K. M., & Richmond, A. D. (2017). Magnetic coordinate systems. *Space Science Reviews*, *206*(1–4), 27–59. https://doi.org/10.1007/s11214-016-0275-y

Liou, K. (2010). Polar Ultraviolet Imager observation of auroral breakup. *Journal of Geophysical Research: Space Physics*, *115*(12), 1–7. https://doi.org/10.1029/2010JA015578

Liou, K., & Newell, P. T. (2010). On the azimuthal location of auroral breakup: Hemispheric asymmetry. *Geophysical Research Letters*, *37*(23), 1–5. https://doi.org/10.1029/2010GL045537

Liou, K., Newell, P. T., Sibeck, D. G., Meng, C. I., Brittnacher, M., & Parks, G. (2001). Observation of IMF and seasonal effects in the location of auroral substorm onset. *Journal of Geophysical Research: Space Physics*, *106*(4), 5799–5810. https://doi.org/10.1029/2000ja003001

Lotko, W., Smith, R. H., Zhang, B., Ouellette, J. E., Brambles, O. J., & Lyon, J. G. (2014). Ionospheric control of magnetotail reconnection. *Science*, *345*(6193), 184–187. https://doi.org/10.1126/science.1252907

Lui, A. T. Y. (1991). A synthesis of magnetospheric substorm models. *Journal of Geophysical Research: Space Physics*, *96*(A2), 1849–1856. https://doi.org/10.1029/90JA02430

Lu, S., Lin, Y., Angelopoulos, V., Artemyev, A. V., Pritchett, P. L., Lu, Q., & Wang, X. Y. (2016). Hall effect control of magnetotail dawn-dusk asymmetry: A three-dimensional global hybrid simulation. *Journal of Geophysical Research: Space Physics*, *121*(12), 11882–11895. https://doi.org/10.1002/2016JA023325

Lu, S., Pritchett, P. L., Angelopoulos, V., & Artemyev, A. V. (2018). Formation of dawn-dusk asymmetry in earth's magnetotail thin current sheet: A three-dimensional particle-in-cell simulation. *Journal of Geophysical Research: Space Physics*, *123*(4), 2801–2814. https://doi.org/10.1002/2017JA025095

McPherron, R. L. (1970). Growth phase of magnetospheric substorms. *Journal of Geophysical Research*, *75*(28), 5592–5599. https://doi.org/10.1029/ja075i028p05592

McPherron, R. L., & Chu, X. (2016). Relation of the auroral substorm to the substorm current wedge. *Geoscience Letters*, *3*(1). https://doi.org/10.1186/s40562-016-0044-5

Mende, S. B., Carlson, C. W., Frey, H. U., Peticolas, L. M., & Østgaard, N. (2003). FAST and IMAGE-FUV observations of a substorm onset. *Journal of Geophysical Research: Space Physics*, *108*(A9). https://doi.org/10.1029/2002JA009787

Milan, S. E., Grocott, A., & Hubert, B. (2010). A superposed epoch analysis of auroral evolution during substorms: Local time of onset region. *Journal of Geophysical Research: Space Physics*, *115*(10), 1–9. https://doi.org/10.1029/2010JA015663

Milan, S. E., Hutchinson, J., Boakes, P. D., & Hubert, B. (2009). Influences on the radius of the auroral oval. *Annales Geophysicae*, *27*(7), 2913–2924. Retrieved from https://angeo.copernicus.org/articles/27/2913/2009/

Østgaard, N., Laundal, K. M., Juusola, L., Åsnes, A., Håland, S. E., & Weygand, J. M. (2011). Interhemispherical asymmetry of substorm onset locations and the interplanetary magnetic field. *Geophysical Research Letters*, *38*(8), 1–5. https://doi.org/10.1029/2011GL046767

Østgaard, N., Mende, S., Frey, H., Immel, T., Frank, L., Sigwarth, J., et al. (2004). Interplanetary magnetic field control of the location substorm onset and auroral features in the conjugate hemisphere. *Journal of Geophysical Research*, *109*. https://doi.org/10.1029/2003JA010370

Østgaard, N., Tsyganenko, N., Mende, S., Frey, H., Immel, T., Fillingim, M., et al. (2005). Observations and model predictions of substorm auroral asymmetries in the conjugate hemispheres. *Geophysical Research Letters*, *32*. https://doi.org/10.1029/2004GL022166

Rostoker, G. (1991). Some observational constraints for substorm models. In *Magnetospheric substorms* (pp. 61–72). American Geophysical Union (AGU). https://doi.org/10.1029/GM064p0061

Tenfjord, P., Østgaard, N., Snekvik, K., Laundal, K. M., Reistad, J. P., Haaland, S., et al. (2015). How the IMF by induces a by component in the closed magnetosphere and how it leads to asymmetric currents and convection patterns in the two hemispheres. *Journal of Geophysical Research - A: Space Physics*, *120*(11), 9368–9384. https://doi.org/10.1002/2015JA021579

Tsyganenko, N. A. (1998). Modeling of twisted/warped magnetospheric configurations using the general deformation method. *Journal of Geophysical Research: Space Physics*, *103*(A10), 23551–23563. https://doi.org/10.1029/98JA02292

Wang, H., Lühr, H., Ma, S. Y., & Frey, H. U. (2007). Interhemispheric comparison of average substorm onset locations: Evidence for deviation from conjugacy. *Annales Geophysicae*, *25*(4), 989–999. https://doi.org/10.5194/angeo-25-989-2007

Wolf, R. A. (1970). Effects of ionospheric conductivity on convective flow of plasma in the magnetosphere. *Journal of Geophysical Research*, *75*(25), 4677–4698. https://doi.org/10.1029/JA075i025p04677

Zhang, B., Lotko, W., Brambles, O., Damiano, P., Wiltberger, M., & Lyon, J. (2012). Magnetotail origins of auroral alfvénic power. *Journal of Geophysical Research: Space Physics*, *117*(A9). https://doi.org/10.1029/2012JA017680